

Investigation of the effects of skewness R_{sk} and kurtosis R_{ku} on tribological behavior in a pin-on-disc test of surfaces machined by conventional milling and turning processes

Elhadji Cheikh Talibouya Ba^a , Marcello Rosa Dumont^a , Paulo Sérgio Martins^b ,
Ramon Martins Drumond^a, Matheus Philippe Martins da Cruz^c , Vitor Ferreira Vieira^b 

^aCentro Federal de Educação Tecnológica de Minas Gerais, Programa de Pós-Graduação em Engenharia de Materiais, Av. Amazonas 5253, Nova Suíça, CEP: 30421-169, Belo Horizonte, MG, Brasil

^bPontifícia Universidade Católica de Minas Gerais, Rua Dom José Gaspar 500, Bairro Coração Eucarístico, CEP: 30535-901, Belo Horizonte, MG, Brasil

^cUniversidade Federal de Minas Gerais, Av. Antônio Carlos 6627, Pampulha, CEP: 31270-901, Belo Horizonte, MG, Brasil

Received: September 22, 2020; Revised: December 01, 2020; Accepted: January 23, 2021

Friction and wear are influenced by the surface conditions of the material, since there is deformation, segregation, generation of oxide films, among others. Roughness is an important characteristic in tribological studies, where the parameters of skewness and kurtosis have greater influence than the conventional parameters R_a and R_q . This study is aimed to investigate the influence of the parameters of skewness R_{sk} and R_{ku} kurtosis on the surface of the US1 AR 360 steel machining by the milling and turning processes in the pin-on-disc sliding wear test. Results showed that surfaces with the same R_a and R_q could be distinguished by the skewness parameter. Different behaviors were observed in the analysis of friction curves, where the skewness effect showed a tendency to reduce the friction coefficient. It was also observed that the feed marks orientation in relation to the sliding direction can influence the tribological behavior of the surfaces.

Keywords: Friction coefficient, Wear coefficient, Roughness, Skewness, Kurtosis, Asperities, Tribology.

1. Introduction

The force of resistance to the relative movement between two bodies in contact is called friction. It is commonly represented by the friction coefficient (μ), the ratio between the frictional force (or tangential force F) and the applied normal load (N). Friction depends critically on the experimental conditions under which it is measured, on the composition and microstructure of the materials present in the tribosystem. In dry sliding tests between metals exposed to air (induces the formation of oxides), generally the friction coefficient can vary from 0.5 to 1.5. In the condition of small loads, μ tends to be low, as the oxides on the bodies surface (and therefore at the contact interface) form a type of protective layer of low shear resistance that limits the growth of joints. With the increase in the normal load, a transition in the friction coefficient is observed, which also increases due to the breakdown of the oxide layer¹⁻³. It is observed that the characteristics of the surfaces have a great influence on the study of friction. As an example, in the absence of external load, the interatomic interactions of the surfaces are capable of causing an adhesive contact between the roughness that contributes to the increase in μ . The deformation of the asperities can be elastic, plastic, viscoelastic or viscoplastic, depending on the contact pressure, roughness and material properties^{1,2}. According to Holmberg and Matthews⁴, in the

contact of two bodies the most relevant properties of the materials are: elasticity modulus (E) that describes the elastic deformation; the hardness (H), which describes the plastic deformation; and the fracture toughness that describes the failure of the material.

Wear is defined as the loss of material or the deformation of the surface of one or both bodies in contact⁵. Like friction, wear is not a property of the material, but a response of the tribosystem. When sliding between surfaces, wear is mainly related to four issues: stresses, thermal effects, chemical reactions and surface interactions. These influences should not be dealt with separately as the contact response between surfaces can change over time. The Archard equation is commonly used to quantify the wear in tribological tests. It relates the volume spent per unit of slip distance (or wear rate Q) with the normal load W , the hardness of the softer surface (H) and K , the dimensionless constant known as the wear coefficient that allows to compare the severity of wear processes in different systems^{2,3}.

The friction curve analysis (*Friction Curve Analysis* - FCA)⁶ is the name given to the measurement and interpretation of the behavior of friction versus time. Require observations about the behavior of the system so that each stage of modification of the surfaces in contact can be correlated with the friction coefficient. The typical friction coefficient curve (Figure 1) between metals, without lubrication, occurs in four stages^{1-3,6}:

*e-mail: cheikh.ba460@hotmail.com

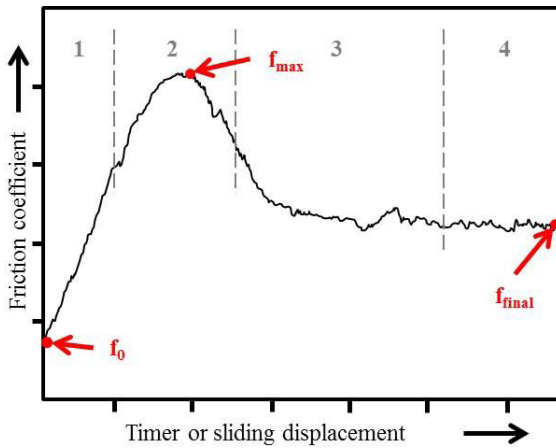


Figure 1. Typical curve of friction coefficient versus sliding time or displacement; Elaboration inspired by ASM¹.

in stage 1, the removal of the surface layer is observed, the increase in adhesion due to the increase in the cleaning of the interfacial areas, the increased interaction between asperities and worn particles, which may gradually increase the value of the friction coefficient. Stage 2 is related to the maximum adhesion, with the deformation of the asperities and an increase in the number of residual particles that increase the wear rate, resulting in the maximum μ peak. In stage 3, there is a decrease in μ , probably due to the formation of a protective tribochemical surface layer or by a decrease in the ploughing and asperities deformation processes. Finally, stage 4 is characterized by the interfacial steady state of tribological conditions, leading to practically constant values of μ as the surface becomes polished.

The roughness manipulation affects the quality of the mechanical and structural components, not only in the visual aspect, but also in the wear and lubrication behavior, friction coefficient, corrosion and fatigue resistance, heat transfer, load transmission, adhesion of coatings and light reflection⁷⁻⁹. Many tribological studies are being carried out to understand the influence of the machining process parameters, and if possible, manipulate them to obtain surfaces with satisfactory characteristics^{10,11}.

The surface characterization by average of roughness is a method widely used in the control of manufacturing processes. In general, the arithmetic average parameter R_a is the most used in industry and scientific studies, mainly in conventional machining processes. It is ideal to relate the effect of the cutting parameters with the surface finish, from the point of view of variations in height and depth of roughness^{7,12,13}. Mathematically, the R_a parameter represents the absolute average of all heights measured along the evaluation length. All valleys must be converted to peaks^{8,14}. This is a justification by which many authors claim that this parameter does not differentiate peaks and valleys. In some cases, small changes in the machining process can be masked by this parameter. Thus, it is recommended to use the quadratic arithmetic average R_q ^{12,15,16}. According to García-Jurado et al.¹³ and Sedlaček et al.¹⁷, R_q is similar to R_a , does not differentiate peaks and valleys, but amplifies (squared) occasional deeper asperities. According to Leach¹⁴,

it is an important parameter for the optical characterization of surfaces.

Stout¹⁸ already mentioned the issue in the industry to determine which parameters would be more appropriate to evaluate the functional performance of a component. Whitehouse¹⁹ drew attention to a more in-depth search, to understand why and to what extent the importance of the roughness reached. It was evident that changes in the R_a and R_q parameters were sufficient to monitor the performance of the manufacturing processes. However, other parameters were needed for further studies, such as corrosion, mechanical strength, optical properties, lubrication, etc. For Todorovic et al.¹², very rough surfaces (elevated R_q or R_a) have less mechanical resistance when compared to “smooth” surfaces. For the study between surfaces in contact, these parameters are not sufficient to obtain reliable answers, this happens because, two surfaces can have the same R_a value, but with different tribological performances, for example. Therefore, parameters are needed to describe how the asperities are distributed along the roughness profile^{9,10,17}. In the study by Liang et al.¹⁶, the surface of six samples of AISI 1045 steel were prepared by dry grinding in order to obtain different roughnesses (R_a , R_q , R_{sk} and R_{ku}). Friction and wear were assessed using the ball-on-disc test equipped with a GGr15 steel ball. As for friction and wear, a possible detail found in the experiment was that the loss is approximately at the same level when the initial roughness is below a certain limit (R_a 0.3 μm to 0.5 μm and R_q 0.1 μm to 0.4 μm). These results indicated that the decrease in R_a and R_q does not bring much benefit to wear resistance when the surface roughness value is low enough.

The skewness parameter R_{sk} (Figure 2a) can be used to distinguish profiles with similar R_a or R_q . A non-Gaussian distribution of the roughness profile is described using R_{sk} and is sensitive to occasional deep valleys or high peaks because it measures the symmetry of the profile distribution over its midline. A symmetric distribution is reflected in zero skewness. Predominant profiles at peaks above a flatter average are reflected in positive skewness, while negative skewness refer to profiles prevalent in deep valleys^{9,20,21}. R_{ku} kurtosis (Figure 2b) describes the probability of flattening the profile. Non-Gaussian surfaces with relatively flat peaks and valleys are reflected in a kurtosis less than 3 (platicurtic), while a kurtosis value above 3 (leptocurtic) indicates sharp peaks and valleys^{9,20,21}. By definition, R_{sk} and R_{ku} represent the quotient between the average values of the ordinates of R_q to the cube and to the fourth power, respectively, in the sampling length^{9,20,21}.

Sedlaček et al.²² investigated the effect of the initial surface roughness on the tribological behavior during the pin-on-disc test in dry and lubricated conditions. The surface of the disc was prepared by polishing and grinding in order to obtain similar values of R_a , but different R_{sk} and R_{ku} . In dry sliding, a reduction in the friction coefficient was observed for surfaces with high values of kurtosis and negative skewness. In the sliding in lubricated condition the relationship between the R_{sk} and R_{ku} parameters with the friction coefficient was the same as for the dry condition, however the effects were more significant. The authors concluded that surfaces with these characteristics have more sites for the storage of wear

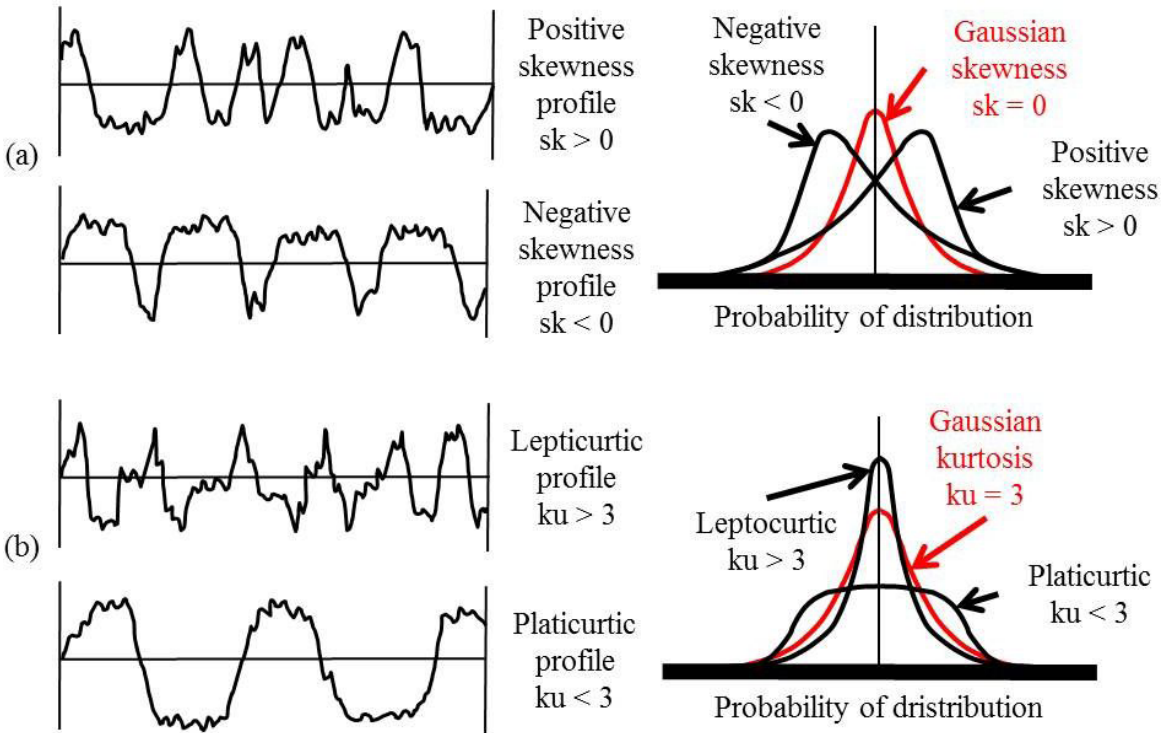


Figure 2. Representation of R_{sk} and R_{ku} parameters; Elaboration inspired by He et al.⁹ and To et al.²⁰.

particles and lubricant. Sedlaček et al.²³ sought to confirm the influence of the skewness and kurtosis parameters of the 100Cr6 steel surface under friction, preparing different surfaces machined by laser, varying the depth and the machining feed rate. The tribological test chosen was the pin-on-disc test, varying the sliding peripheral speed with constant load. It was found that, increasing the feed from 125 μm to 500 μm , S_{sk} was reduced by 4.3 times and S_{ku} increased by almost nine times, which resulted in a 25% reduction in the friction coefficient. Shi et al.²⁴ carried out a mathematical study of the effect of roughness (R_q , R_{sk} and R_{ku}) on the fatigue life of a spherical bearing under severe working conditions (loading and rotation). The results showed that the surface resistance is improved when R_{sk} is negative and R_{ku} is close to or below three. According to the authors, the negative skewness reflects a surface with greater lubricant retention capacity. Dzierwa²⁵ evaluated the influence of 42CrMo4 steel surface preparation on friction and wear in the tribological ball-on-disc test using a 100Cr6 steel ball. The discs were prepared to obtain surfaces of a similar arithmetic average range of height S_a . Results showed that the strongest relationship between wear and surface topography was attributed to the skewness parameter S_{sk} . The wear volume was proportional to the value of the S_{sk} . It was also observed that higher values of kurtosis led to lower values of volumetric wear.

Grabon et al.²⁶ report that the orientation of asperities in relation to the sliding direction has an important influence on the behavior of the friction coefficient and the wear of a tribosystem. The parallel and perpendicular orientations are extreme opposite conditions^{26,27}, but intermediate angles are generally used for the manufacture of burnished

surfaces of cylinders used in internal combustion engines, for example. In general, studies carried out in this area show that oil consumption is reduced when the burnishing angle is increased. In the study by Yuan et al.²⁷ a significant reduction in the friction coefficient was observed in the tribosystem composed of a textured surface and oriented perpendicular to the direction of the reciprocal sliding, when compared to the tribosystem composed of a “smooth” surface. However, when comparing the extreme orientations (parallel and perpendicular), different results were obtained, leading to the question: which of these conditions is the best? From the other analyzed results, it was concluded that the best tribological conditions, in terms of friction coefficient, were obtained for orientations between these extremes: in general 30° and 60°.

In this study, the influence of the roughness parameters R_{sk} and R_{ku} on the surface of the USI AR 360 steel were investigated by the conventional turning and milling processes in the tribological test of sliding pin-on-disc. The friction and wear coefficients K were evaluated in three sliding tracks of each machining disc. The tests were parameterized with a normal load of 5 N, peripheral speed of 0.2 ms^{-1} and 15 minutes of sliding. Statistical data analysis techniques were used to assess the occurrence of significant differences in the parameters covered between the studied surfaces.

2. Materials and Methods

The material used for this study was USI AR 360 steel, whose reference information (manufacturer and other suppliers) of chemical composition and hardness are presented in Table 1. This material is applied for structural

Table 1. USI AR 360 steel proprieties.

C max.	Mn max.	Chemical composite (%)			S max.	Others	Hardness HB
		Si max.	P max.				
0.22	1.5	0.40	0.030	0.015	Cr - 0.80	360	
					Mo - 0.40		
					Ti - 0.030		
					B - 50 ppm		

Table 2. Identification of the discs and tests realized.

Order of test	Pin	Disc	Identification of the sliding track radius	Identification of the test
1°	P1	Milled (F)	23	F23
2°	P2		18	F18
3°	P3		13	F13
4°	P4	Turned (T)	13	T13
5°	P5		18	T18
6°	P6		23	T23

purposes of high resistance to wear and abrasion: tractors, backhoes, rail coverings, ore conveyors, blast furnace parts, industrial fans, among other applications. The choice of this material was due to the motivation to study a material that is still little mentioned in the literature, and this study can then contribute to the scientific research data collection. Two discs were prepared by means of facing operation in conventional machining processes, one by milling and the other by turning. The machine tools used were the Manrod MR-205 bench drill-milling machine and the Veker TVK-1224ECO bench turning machine. The surfaces were machined to obtain R_a and R_q statistically equal with 95% reliability, thus evaluating the influence only of the R_{sk} and R_{ku} parameters on the friction and wear behavior in the tribological test^{22,25}. The initial roughness was measured with the Mitutoyo SJ-210 portable roughness meter, Gauss filter, 0.5 mm/s of measure speed and five length samples (cut-off) with 0.8 mm.

In total 10 roughness measurements were made in different positions on the surfaces to calculate representative arithmetic average values. The Shapiro-Wilk's W test of normality was applied to each population, respective to each machined surface, to assess the distribution of data in relation to the normal probability distribution. From the result of the normality test, it was possible to define the correct use of statistical tests to assess significance (hypothesis test) between the representative values of each population: Student's T test (parametric), Mann-Whitney U Test (nonparametric) and Kruskal-Wallis ANOVA test (nonparametric)²⁸. A 95% reliability parameter was considered for all the analyses made.

The pin-on-disc sliding wear test was performed on the Microtest SMT-A/0100-MT/60/NI equipment, based on the ASTM G99-05²⁹ standard, whose parameters were: dry sliding, room temperature of approximately 20°C, air relative humidity between 40% and 50%, normal load of 5 N, peripheral speed of 0.2 ms⁻¹, three wear tracks per disc and 15 minutes of sliding. Altogether, six carbide pins (K10, 92% WC, 6% Co, 1650 HV) with 3 mm tip radius were used, one for each track. The different results of the tests were identified from the runway radius value (13 mm, 18 mm

and 23 mm) and from the disc facing process (F = Milling and T = Turning), shown in Table 2.

Due to the objective of evaluating the influence of the roughness of the machined surfaces, it was then decided to use the lowest load available on the equipment in such a way that the roughness resulting from the machining processes could withstand the loading in relative motion as long as possible. Once the asperities were removed, that is, the formation of a new surface, the study would no longer have the proposed relevance. In order to reduce the interference of the effects of temperature on the contact interface of the tribosystem, such as increasing the rate of oxide formation and reducing the mechanical resistance of the material by microstructural modifications, as well as being governed by the cutting speed in the machining of the materials, it was decided to use a low peripheral speed that was also similar to other studies, such as Sedlaček et al.²², Sedlaček et al.²³, Dzierwa²⁵ and Dzierwa et al.³⁰.

Preliminary tests were carried out to observe the time necessary for the friction coefficient to reach steady state, so it is not necessary to prolong the unit tests by more than 15 minutes, because changes in friction coefficient after running-in and steady state regimes could be related to a new surface formed due to prolonged wear. This time was enough to reach a constant sliding distance of 180 meters on all the tracks analyzed. In the studies carried out by Sedlaček et al.²³ and Sedlaček et al.³¹, a constant value of 100 meters for the sliding distance was sufficient for the analysis of the results. In the study by Dzierwa²⁵ the unit tests were performed in 3 minutes, enough time for the friction coefficient to reach steady state. Dzierwa¹⁰ kept the sliding distance constant at 282.6 meters, equivalent to a time of approximately 30 minutes. In his results, the author stated that after reaching the steady state, the friction coefficient value was similar for all tribosystems analyzed, being more important to analyze the behavior of the friction coefficient in the running-in regime and its transition to the steady state.

The dimensionless wear coefficient K was calculated using the Archard equation (Equation 1), whose worn volume per sliding unit (Q) was measured indirectly through the loss of mass.

$$K = \frac{\Delta m \times H}{\rho \times L \times W} \quad (1)$$

The specific mass ρ of each disc was calculated using geometry and mass, both measured after machining processes. The H hardness of the USI AR 360 steel shown in Table 1 was converted to Vickers hardness using conventional tables, adopting a value of 380 HV. The normal load W of 5 N, expressed in kilogram force, was kept constant in the equation. The linear sliding distance L , in meters, was calculated from each lane radius (R13, R18 and R23), the sliding time and the peripheral speed. At the beginning and end of each test, the mass variation Δm , expressed in kilograms, was calculated from the measurement of the initial and final masses, respectively. Arithmetic average values of mass were considered from 4 replicates measured on the Shimadzu AX 200 precision scale, with 0.0001 and 0.001 grams of resolution and error, respectively. The specimens were submerged in a thinner bath in an Elmasonic S 10H ultrasonic cleaner. The variation in the mass of the discs and pins, the friction and wear coefficients K were also statistically evaluated as well as mentioned on the roughness. After the tests, SEM and EDS analysis of the pins and wear tracks were performed on the JEOL equipment, model JSM-IT300.

3. Results and Discussion

Table 3 shows the physical characteristics of the discs prepared for the tests. The results obtained were considered satisfactory for the test. According to the ASTM G99-05²⁹ standard, the diameters and thicknesses obtained are within the recommended range. The biggest difference observed between the discs was the mass, 7.4321 grams, which, however, could not be considered harmful to the studies. The difference in mass occurred due to the different diameters of the discs. On the other hand, the specific mass calculated for both discs was the same, that is, both discs are made of the same materials, allowing the discussion of tribological behavior to be restricted to the surface characteristics of the discs.

In Figure 3, the appearance of the faced surfaces of the discs is presented when compared to the “fingerprints” of the turning and milling processes.

The surface finish of the discs is different due to the different feed marks made by the cutting tool during machining. In turning (Figure 3a), the cutting edge follows a straight path perpendicular to the rotation axis where the disc²¹ is fixed. The feed marks are then similar to successive circles whose radius decreases as the cutting edge approaches the center of the face. But in the real process the impression left on the surface has a spiral shape. For the milling process

Table 3. Physical characteristics of the discs.

Characteristics	Milled	Turned
Diameter (mm)	55.82	57.15
Medium thickness and standard deviation (mm)	7.20 ± 0.01	7.21 ± 0.02
Parallelism tolerance between the faces (mm)	0.03	0.05
Mass and standard deviation (g)	136.7570 ± 0.0004	144.1891 ± 0.0007
Specific mass and average value (kg/m ³)	7778.79	

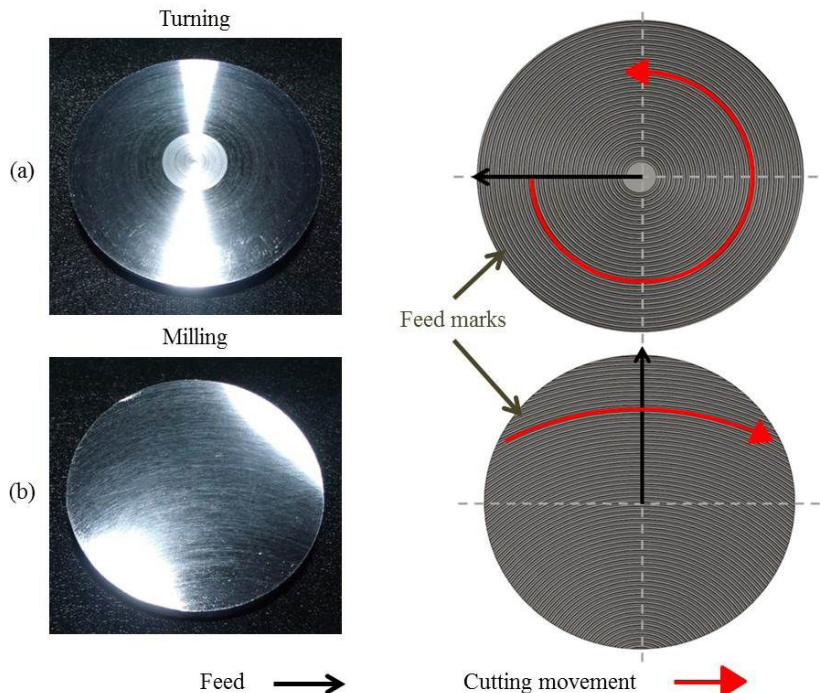


Figure 3. Preparation of the discs for the sliding test with illustration of the feed marks printed on the surface in relation to the turning (a) and milling (b) processes.

(Figure 3b), the cutting edges execute the cutting movement (rotation) while the disc, fixed on the table, moves in a straight path perpendicular to the axis of rotation of the tool²¹. The feed marks rates are similar to arcs whose length refers to the unit length of contact between the cutting edge and the machined surface. In the illustrated case, the diameter of the tool is greater than the diameter of the machined part.

3.1 Initial surface roughness

The measured arithmetic average values with their respective standard deviations for R_a , R_q , R_{sk} and R_{ku} are shown in Table 4 together with the results of the significance tests when comparing the machining processes.

By average of 10 measures carried out on each surface, the average roughness results indicated that the goal of preparing the surfaces was successfully achieved. The parameters of R_a were 0.50 and 0.48 μm for the milled and turned discs, respectively. The difference of 0.02 μm between the values was not significant, firstly by the standard deviation values that indicated an overlap of the dispersion of the values and secondly, this hypothesis is confirmed by the significance test value (p-value) that was 0.572, which is above 0.05 (p-reference value)³². Barányi³³ also obtained a similar arithmetic average roughness, however three-dimensional, between surfaces facing by milling and turning, 1.56 and 1.55 mm respectively. Kurtosis values remained below 3, while skewness was positive. The authors did not report standard deviation, but apparently the values of skewness and kurtosis of the milled surface were higher in relation to the turned surface. From this, it is noticed that the parameters of skewness and kurtosis, as well as R_a and R_q , can be modified by varying the machining parameters

of the same process: feed, cutting speed, cutting depth, tool geometry, among others¹⁸. Horváth et al.³⁴ investigated the influence of machining parameters (feed, cutting speed and cutting depth), the geometry of the cutting tool and the silicon content on the roughness (R_a , R_z , R_{sk} and R_{ku}) during the turning of Al-Si. Two tool geometries were used, one conventional (ISO standard) and another Wiper (Figure 4). Results showed that R_a and R_z were the only dependent parameters for all input variables of the study. R_{sk} and R_{ku} showed significant differences only related to the geometry of the tool. According to the authors, an ideal surface for tribological applications (negative skewness and kurtosis above three) could be obtained by turning using the Wiper geometry tool. The reduction of the secondary position angle makes the secondary cutting edge more effective in machining: after the passage of the main edge (primary cut), the secondary one promotes a “fine cut”, or a “smoothing”, possibly removing the higher peaks of the machined surface. From this, it is clear that the skewness parameter can be reduced.

The average parameter R_q of 0.60 μm shown in Table 3 was obtained on both surfaces, and like R_a , it did not show any significant difference (p-value of 0.699). This result was expected because these parameters are similar, they do not differentiate peaks and valleys, however R_q amplifies occasional deeper asperities^{13,17}. The skewness parameter obtained on the surfaces was 0.10 and 0.21 respectively machined by milling and turning. It is interesting to note that the results would be considered similar when analyzing only the measurement deviations obtained. However, the calculated p-value showed that the values were statistically different, thus differentiating the roughness profiles with similar R_a and R_q . Figure 5 shows

Table 4. T significance test of the average roughness values R_a , R_q , R_{sk} e R_{ku} .

Variable	N° of specimens	Milling average value (μm)	Turning average value (μm)	Milling standard deviation (μm)	Turning standard deviation (μm)	T Student p-value
R_a	10	0.50	0.48	0.01	0.04	0.572
R_q		0.60	0.60	0.10	0.05	0.689
R_{sk}		0.10	0.21	0.13	0.16	0.013
R_{ku}		2.74	2.73	0.29	0.20	0.937

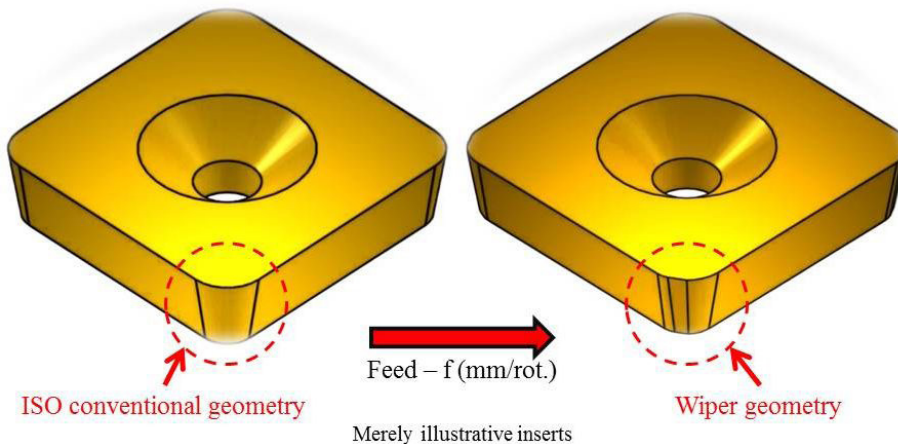


Figure 4. Comparison between ISO and Wiper cutting edge geometries of a hypothetical insert.

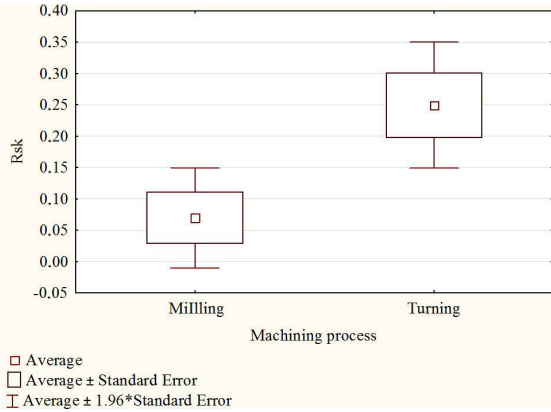


Figure 5. R_{sk} arithmetic average and dispersion obtained in machining processes.

the results of R_{sk} graphically comparing the two processes. The milled surface showed 50% less skewness in relation to the turned surface, indicating less peaks.

The kurtosis of both machined surfaces was statistically similar, with an arithmetic average value of 2.7 and a p-value of 0.937. The R_{ku} value, less than 3, indicates a greater flattening of the peaks and valleys. This result suggests that R_{sk} can be used to differentiate the roughness profiles between the two machining processes used. The values of R_{sk} and R_{ku} were within the range specified by Stout¹⁸, of R_{sk} between 0.2 and 1.0 and R_{ku} between 2 and 4 for turning and of R_{sk} between 0.2 and -1.6 and R_{ku} between 2 and 10 for milling. It is worth mentioning here that the measurement deviations obtained for skewness and kurtosis were of the same order of magnitude as the average values, indicating that there was greater dispersion compared to the parameters of R_a and R_q . Attention must be paid to the use of skewness and kurtosis. Some studies have shown that these parameters can be accompanied by significant uncertainties, mainly because they are mathematically related to R_q through potentiation¹⁰. García-Jurado et al.¹³ studied the influences of the cutting parameters (feed, cutting speed and cutting depth) on the roughness (parameters R_q , R_{sk} and R_{ku}) and indirect/secondary adhesion during dry turning of an Al-Cu alloy. The authors made the following conclusions regarding roughness: (1) at constant cutting speed, R_q and R_{sk} are proportional to the feed. For R_{ku} the relationship is the opposite; (2) keeping the feed constant, R_q tends to decrease with increasing cutting speed. R_{sk} and R_{ku} showed no linear trend. Limandri et al.³⁵ conducted a study on the superficial characterization of dental enamels in patients of various ages. The parameters S_a , S_q , S_z , S_{sk} and S_{ku} were measured. In their results, the authors only described the surfaces, in terms of skewness and kurtosis, according to theory and other studies, and no more than that. As a justification, measurement uncertainties above 100% were observed for these parameters. The authors concluded that S_{sk} and S_{ku} are not recommended for this type of study.

3.2 Friction coefficient curves analysis

In Figure 6, the friction coefficient versus number of revolutions curves in the tribological test for the three tracks of each disc are presented, whose objective was to

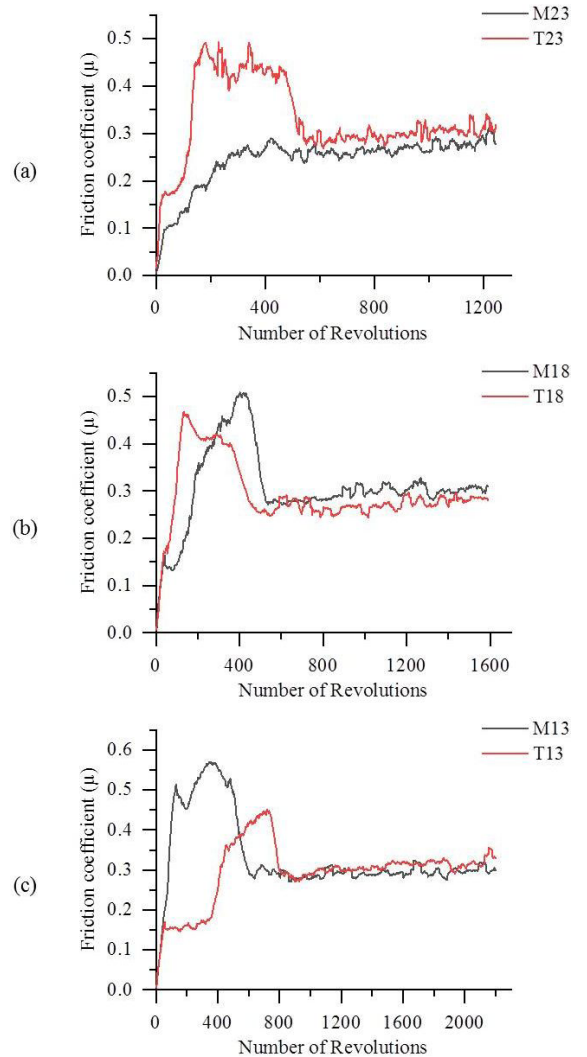


Figure 6. Friction coefficient curves, tracks R23 (a), R18 (b) and R13 (c).

investigate possible influences of roughness, in particular the parameter R_{sk} , which according to Blau⁶ is related to the microcontact in the tribosystem interface. There were different initial behaviors of the friction coefficient and soon after, its stabilization, making it possible to distinguish the phases of running-in and steady regime³⁰.

The curve of the F23 test differs, according to Blau⁶, from a surface contaminated by particles of low shear resistance that form a protective film. In the case of the surface with fewer peaks (lower R_{sk}), these particles are expected to accommodate more easily in the voids between the valleys, and thus acting as a boundary lubrication²³. The subsequent increase in the friction coefficient happened because of the joints growth at the interface, until reach the real contact area necessary for normal load starting the steady regime. In T23, two periods of transition and stabilization are observed during the “running-in”. In stabilization, it is necessary to have a protective oxide layer, supported by the surface, whose low shear resistance keeps friction low. In the transition,

the increase in friction occurs due to the breaking of this layer, deformation and breaking of the asperities. Then, μ remains approximately constant at a higher value, probably due to the presence of debris (wear particles) at the interface without joint growth. In the next transition phase, debris are removed from the interface and a real contact area can be formed, ending and stabilizing friction. As this surface has a larger R_{sk} than the milled one, it is assumed that there is less capacity for retaining debris and/or greater formation of it, causing them to remain in the contact interface for a longer time²³. This change in regime is possibly due to the growth of fatigue cracks subsurface that leads to the appearance of debris that modifies the tribological system, from two to three bodies³⁶. Curves F18 and T13 can be interpreted similarly to T23, except for some particularities. In the T13 curve, it is observed that a probable initial oxide layer remained for a longer time at the interface (up to 300 revolutions) than in F18 (up to 100 revolutions). In addition, on T13 curve has the longest running-in time (up to 900 revolutions) than in F18 (up to 550 revolutions). This leads to the hypothesis that R_{sk} has an influence on the time required for the friction coefficient to reach the steady state¹⁶. In curves T18 and F13 the interpretation approaches the typical friction curve between metals^{1-3,6}, with a gradual growth in friction resulting from the great interaction between the roughness and impurities present at the interface. Then, the surface becomes smoother, a real contact area becomes necessary for the load, the wear is reduced and consequently the friction³⁰.

Table 5 shows the arithmetic average values of friction coefficients in the steady regime and the results of standard deviation. Table 6 shows the Mann-Whitney U significance test of the friction coefficient. The results show that the averages were statistically significant with p-value below 0.05³². Of the three sliding tracks, radius 23 (R23) and 13 (R13) showed lower friction coefficient for the milled surface compared to the turning. In relation to the higher value, in the R23 lane there was a difference of 9%, 11% in the R18 lane and 2% in the R13 lane.

These results may be related to the skewness parameter that distinguishes the roughness profile of the analyzed surfaces. A difference of 50% in R_{sk} (results shown in Table 4 and Figure 5) shows that the turned surface has

a greater number of peaks projected above the midline of the roughness profile³⁷. The actual contact area decreases, as the skewness profile becomes increasingly positive³⁷⁻³⁹. During the accommodation of the surfaces along the relative movement, the contact pressure decreases due to the increase in the real contact area. Since the highest peaks do not have sufficient mechanical strength to withstand the normal load imposed on the tribosystem in an elastic deformation regime, then the greater formation of wear particles acting on the interface and/or the predominance of accentuated plastic deformation in asperities³⁷ can be expected. When compared to the surface with less skewness, these factors can provide a greater friction coefficient (in running-in and steady state) and prolong the time necessary for the transition of the friction regime to occur. Surfaces whose roughness profile has fewer peaks above the midline of the roughness profile may have a greater ability to retain impurities or debris from the breakage of the oxide film that could act at the interface as a third abrasive body. Yan et al.³⁷ also mention that an increase in skewness in the roughness profile can lead to a reduction in the fatigue resistance of surfaces.

When investigating the influence of skewness and kurtosis parameters on the friction coefficient in dry sliding, Sedlaček et al.¹⁷ showed that, in general, surfaces with high S_{ku} and more negative S_{sk} tend to reduce the friction coefficient. In the study presented by Sedlaček et al.³¹, comparing the tribological performance of a turned surface and a laser textured surface, both presented similar S_a , S_q and S_{ku} parameters, being then differentiated by the skewness: S_{sk} of the textured surface was nine times smaller than the turned surface. This difference resulted in a 30% reduction in the friction coefficient in relation to the turned surface. In lane R18 (Table 5), the controversial result of the friction coefficient greater than on the turned surface may be related to different local characteristics of the roughness, contrary to the statistical results, or the greater presence of debris as explained in the F18 curve of Figure 6. The average time required for friction to reach steady state was estimated, being 5.50 minutes for the milled surface and 5.63 minutes for the turned one. On the milled surface, the stabilization of the microcontact at the interface would occur more quickly due to the lower presence of high peaks that could contribute

Table 5. Descriptive statistic of the friction coefficient in a steady state.

Tests	Nº of specimens	Average Friction coefficient (μ)	Standard deviation (μ)
F23	172	0.280	0.012
T23		0.308	0.012
F18		0.303	0.009
T18		0.269	0.011
F13		0.288	0.011
T13		0.293	0.009

Table 6. Mann-Whitney U test of wear coefficient significance.

Track	Nº of specimens	Positions sum (ranking) Milling	Positions sum (ranking) Turning	U factor calculated	p-value
R23	172	16253.000	43087.000	1375.000	0.000
R18		44068.000	15272.000	394.000	0.000
R13		25720.000	33620.000	10842.000	0.000

to the formation of wear particles. However, the suggested hypothesis cannot be confirmed since the time difference was not statistically significant. Liang et al.¹⁶ observed that in the increment of R_{sk} , the friction coefficient increases and the transition time of initial wear decreases.

In addition to the skewness magnitude, the orientation of the asperities in relation to the sliding direction of the pin could have interfered in the behavior of the friction coefficient. Charsetad and Khorsandijou⁴⁰ studied the influence of the magnitude and direction of roughness under the friction coefficient on dry contact between two equal metals with similar roughness. The authors concluded that the friction coefficient depends on the surface roughness and the contact direction of the roughness. In the study by He et al.⁹, surfaces were textured with different parameters to investigate the influences of S_{sk} and S_{ku} on the friction coefficient. The authors were unable to extract correlations between the texturing angles (0° , 45° and 90°) and the skewness and kurtosis parameters on tribological performance. A possible explanation of the orientation influence of the feed marks is presented with the help of Figure 7.

Figure 7 illustrates a simple modeling of the contact interface in the pin-on-disc test. It is assumed that both surfaces are machined under similar parameters in terms of cutting geometry, feed and cutting depth. The pin with a

3 mm nose radius penetrates 0.10 mm over the surfaces of both discs and travels a radial path of 7 mm in 360° . The feed marks referring to the turning remain in the same direction of sliding of the pin, while on the milled surface the feed marks vary between 0° to 90° . The wear track (marked in blue in Figure 7) on the surface of the disc is formed over time after the application of a normal load on the pin and a rotary movement with an established speed. Based on the μ results (Table 5), when the roughness follows the same direction as the sliding, the contact surface of the pin is probably sustained constantly by a support length, similar to a guide rail. As the sliding time increases, the width of the "rail" increases (flattening of the asperities), thus increasing the friction coefficient, which would be greater in relation to the milled surface where the contact would prevail intermittently, since the orientation of the "rail" does not remain constant. Moronuki and Furukawa⁴¹ investigated the effect of perpendicular and parallel orientation of asperities on the behavior of the friction coefficient. Through the results it was observed that the friction coefficient showed greater stability and less magnitude when the asperities of the analyzed surface was oriented perpendicular to the sliding direction of the counterbody. The authors stated that in this condition the real contact area was minimal, and with that, the adhesion strength was also minimal. Pettersson and

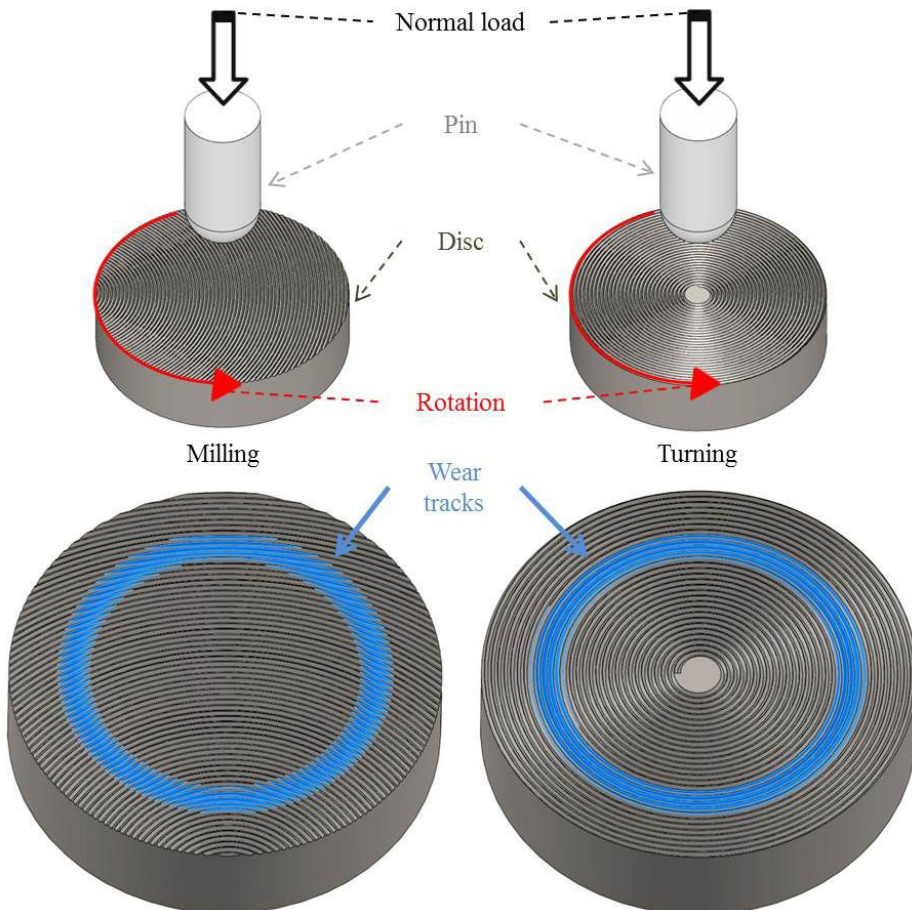


Figure 7. Illustrative modeling of the wear tracks produced in the pin-on-disc test.

Jacobson⁴² carried out tribological studies on surfaces of a silicon substrate coated in DLC (Diamond-Like Carbon) during the reciprocal sliding test in a boundary lubrication regime. The authors also observed better results on the surface whose asperities were oriented perpendicular to the direction of sliding. According to the authors, in this tribosystem the intermittent contact between the surfaces made it easier for the lubricant to penetrate the contact interface. On the other hand, asperities oriented in parallel to the sliding direction provided a continuous contact between the surfaces, which hindered the lubricant's action and increased the adhesion at the tribosystem contact interface.

3.3 Wear coefficient K and specimens analysis

The wear coefficient K was calculated by the loss of mass of the discs after each sliding test. Using the Archard equation⁶, the K value was obtained by calculating the wear rate Q of the three sliding tracks. The total arithmetic average values of all tests are presented graphically in Figure 8, whose K values were respectively $5.24E-10 \pm 4.59E-10$ and $3.46E-10 \pm 3.68E-10$ for the surfaces facing milling and turning.

Taking into account the Archard equation, it appears that the load W was the main responsible for the magnitude of wear presented in the tests. The values were lower than the value considered as "moderate wear" (K between 10^{-8} to 10^{-4}) according to Bhushan², with a wear coefficient K in the order of 10^{-10} . According to the author, the wear coefficient can be interpreted as the probability of transferring a fragment of material or the formation of a wear particle from a contact between asperities. In the "moderate wear" range, the contact interface is altered by the presence of oxide particles that are less aggressive when compared to the wear particles formed by the surface roughness crack. Oxides can also contribute to the temporary reduction and/or stabilization of the friction coefficient, as mentioned earlier in the discussion of friction curves^{3,36}. Although the result

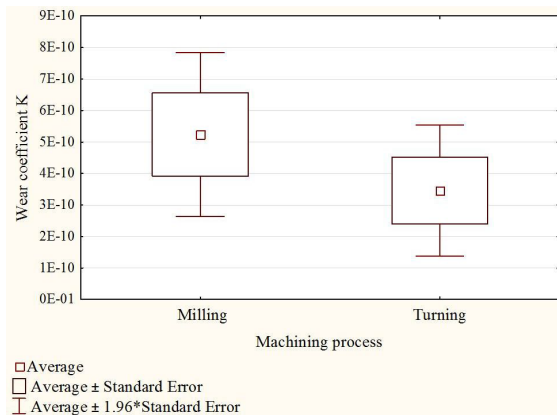


Figure 8. Wear coefficient K arithmetic average and dispersion calculated after the pin-on-disc test.

is statistically insignificant according to the p-value above 0.05 presented in Table 7, in Figure 8 there was a tendency to reduce the K coefficient in the turned surface, whose R_{sk} was greater. The turned surface showed an average wear coefficient 33.5% lower than the milled surface.

Considering that the friction coefficient on the milled surface prevailed lower (Table 5), there is then the possibility of a difference in the energy dissipation mode. According to Blau⁶, a high friction value does not necessarily imply high wear because the energy dissipation mode can be different from one tribological system to another. This energy can be used, for example, to form oxides, to scratch, to form cracks, to heat the surface or to cut the layers of debris. There is a hypothesis that on the turned surface the energy dissipation was distributed between the crack of oxide layers and the deformation of the asperities. On the milled surface, the energy dissipation may be majorly concentrated on the deformation of the asperities, even because the orientation of the feed marks are not in the same direction as the sliding, that is, the action of shearing the asperities will be greater when they are not parallel to the sliding. However, other characterization techniques would be necessary to obtain more robust answers on this subject. Another hypothesis for the result of the wear coefficient would be related to the indirect determination of the worn volume through the loss of mass of the discs. The reduction in mass was very small in relation to the total mass of the discs, and possibly the resolution of the precision balance was not sufficient to measure the real mass. The profilometry technique, for example, would be more recommended, as the worn volume is calculated directly. In the study by Dzierwa et al.³⁰, the wear volume, measured by profilometry, was lower on surfaces that showed less S_{sk} . According to the authors, the roughness profile constituted by a greater number of valleys can provide less wear due to the reduction of plastic deformation and/or crack of asperities that are above the midline of the profile. It was also mentioned that, from a tribological point of view, skewness is more important than kurtosis. From the analytical study carried out by Ghosh and Sadeghi³⁹, it was observed that the wear rate is higher the more positive the skewness of the roughness profile, as the contact pressure has a positive correlation with the skewness.

SEM and EDS analysis were performed on the contact surfaces of all pins in order to obtain a better study about the influence of the R_{sk} parameter and also the orientation of the asperities. More expressive differences were obtained in the pins used in lanes R13 (Figure 9).

On both pins, the contact area is identified by the dark gray edges in an elliptical form. The F13 pin showed a greater wear area when compared to the T13 pin, with a difference of 68%, with the F13 pin as a reference. Interesting fact is that in this wear track the difference in friction coefficient was the smallest (2% statistically significant) found in the tests (Table 5). Through EDS area analysis (spectra 5 and 11) it was possible to verify the majority of chemical elements

Table 7. Mann-Whitney U test of wear coefficient significance K.

N° of specimens	Positions sum (ranking)		U Factor Calculated	p-value
	Milling	Turning		
12	170.000	130.000	52.000	0.260

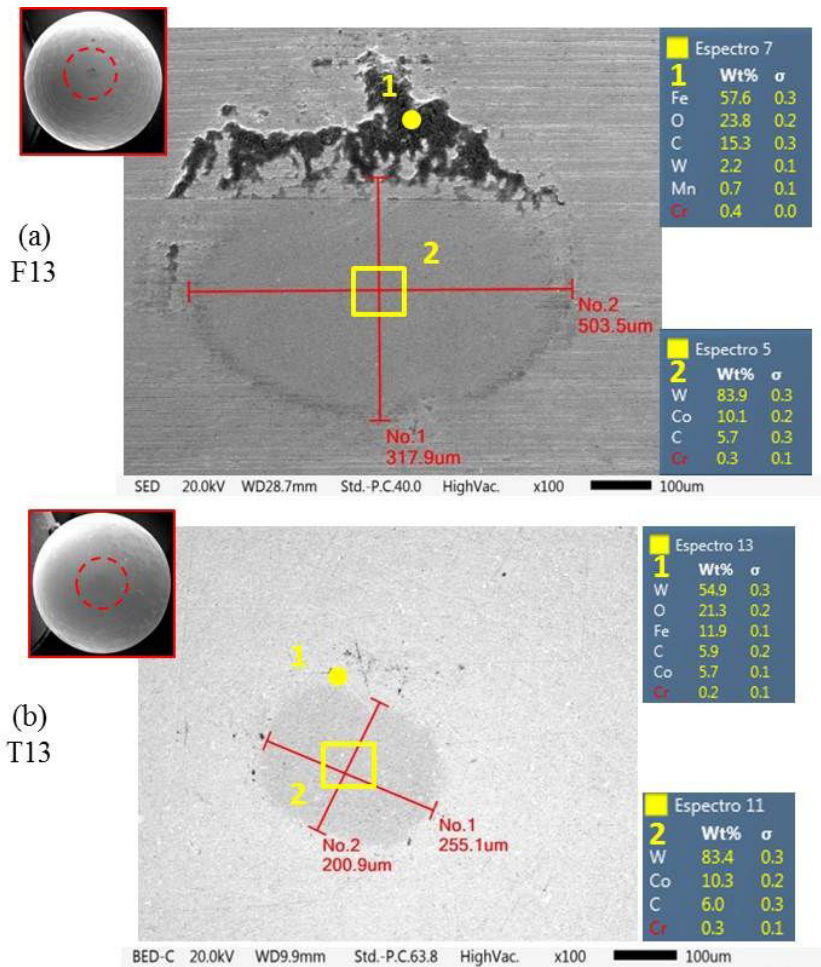


Figure 9. SEM and EDS analysis of the wear pins used in the R13 tracks: pins P3-F13 (a) and P4-T13 (b).

present in the composition of the carbide pin, and therefore, there is no clear evidence about the presence of adhesive wear. In a punctual analysis (spectra 7 and 13), pin F13 showed the adhesion of a dark layer composed mainly of iron and oxygen, that is, probably an oxide layer accumulated during the test⁴³. In pin T13 it was also found the presence of iron and oxygen, but in a smaller concentration, but no oxide layer was observed. This can prove the hypothesis mentioned above for the results presented on the wear coefficient in Figure 8 and Table 7, where Blau⁶ states that tribosystems with similar friction coefficients can have totally different wear behaviors due to the energy dissipation modes. In this case, it can be assumed that there is a greater presence of oxides acting in the tribosystem composed of the milled surface and, at the same time, a greater contact area at the interface, possibly due to the feed marks orientation of the machining process, which has also been discussed previously.

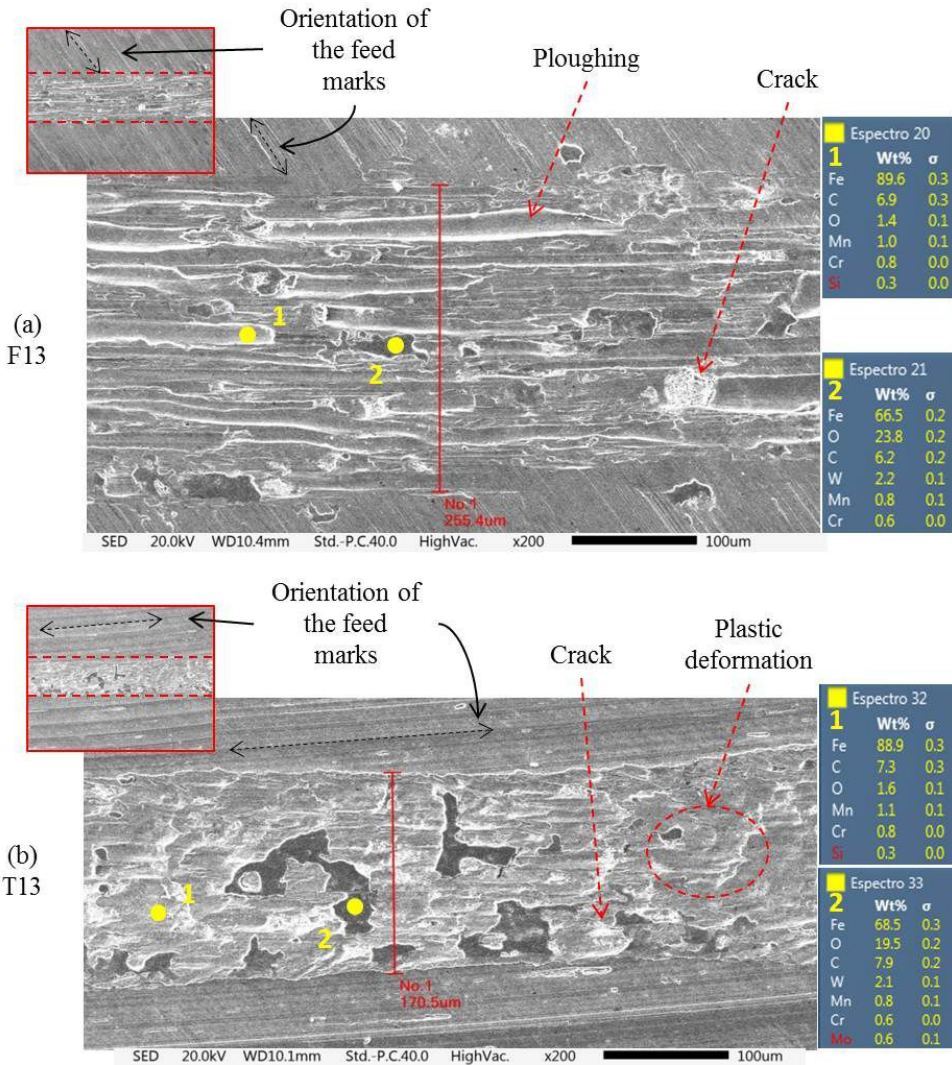
To finalize the wear analysis on the pins, the arithmetic average variation of mass Δm was calculated for each replica of mass measured in the tests. As shown in Table 8, the values are in the order of 10^{-4} grams, close to the resolution and 10 times below the measurement equipment error. The statistical analysis of the results showed that there was no

significant difference in mass variation between the tests. From the statistical results of the mass variation analyzed between the tests, it is not possible to state the occurrence of significant wear on the pins. The results are consistent with the wear coefficients shown in Figure 8, where the wear was classified as below moderate², predominant of oxidative wear. A similar analysis was cited by Dzierwa et al.¹⁰ and Dzierwa et al.³⁰, where they verified that the magnitude of the wear of the pins (considering it to be the hardest material) is smaller, however it is an indication of the magnitude of the wear of the sliding tracks.

The SEM and EDS analysis on the R13 wear tracks after the tests are shown in Figure 10. At first it is possible to notice the predominance of different wear mechanisms between the surfaces, which have been totally modified in relation to the initial finish (region off the runways). The black arrows identify the feed marks orientation of the machining processes in relation to the wear tracks, as discussed in Figure 7. In the section observed in the F13 track, the feed marks are oriented at an angle between 0° and 90° , apparently close to 45° . In T13 track, however, a greater similarity is observed with the feed marks orientation produced in turning. By measuring the width of the tracks, it was possible to

Table 8. Kruskal-Wallis significance test of mass variation of the wear pins.

Kruskal-Wallis test: $H(5, N=24) = 4,6272$						
Pins identification	N° of specimens	Mass variation (g) Average	Standard deviation (g)	Positions sum (ranking)	Positions average (ranking)	p-value
P1-F23	4	0.0001	0.0001	46.5000	11.6250	0.4630
P6-T23		-0.0001	0.0001	27.5000	6.8750	
P2-F18		0.0001	0.0001	48.5000	12.1250	
P5-T18		0.0001	0.0001	57.5000	14.3750	
P3-F13		0.0002	0.0002	66.0000	16.5000	
P4-T13		0.0001	0.0002	54.0000	13.5000	

**Figure 10.** SEM and EDS analysis of the R13 wear tracks F13 (a) and T13 (b).

observe the correlation with the magnitude of the wear of the pins (Figure 9)^{10,30}. F13 and T13 tracks showed values of approximately 255.4 μm and 170.5 μm, respectively. In the spectra of the spot analysis of EDS it was possible to observe major intensities of the chemical elements present in the composition of the steel USIAR 360. Spectra 21 and 33 of the tracks F13 and T13 respectively, indicated by point 2 are located in darker regions where there was greater intensity of oxygen. This may be associated with a slight localized

oxidation, which was also observed by Souza et al.⁴³. In these spectra, small intensities of tungsten were also observed, a major element of the chemical composition of the pins, assuming then that there was a small loss of material due to the relative movement of the surfaces.

In F13 the wear showed an abrasive predominance marked by the ploughing oriented in the direction of the relative movement between the surfaces. The asperities of the harder material (the pin) acts as a micro cutting edge,

similar to conventional machining processes. Under the action of normal loading, the plastic deformation of the less hard surface allows the penetration of the harshest asperities. Adding the relative movement shortly thereafter, perpendicular to the loading direction, the shear then begins with removal of material from the surface^{10,30}. In the T13 track, regions that were plastically deformed in the direction of sliding of the pin and craters were observed, resulting from the crack of the asperities joints and subsequent crack of surface material, with plastic deformation and adhesion being the predominant mechanisms in wear⁴⁴. In the study by Souza et al.⁴³ a surface of AISI 4340 steel was submitted to the pin-on-disc test in relative motion with a pin coated by TiAlN where the wear produced was similar to that shown in Figure 10b. According to the authors, wear was considered the most severe. This statement can be valid for the present study when considering the general results of the friction coefficient associated with differences in surface skewness (Table 6) and the discussion held about the feed marks orientation in relation to sliding (Figure 7). It is also worth mentioning that the concept of wear is not restricted to material loss, which was not observed with relevance in the results of the wear coefficients shown in Figure 8. In this study, the concept of wear was predominantly directed to the geometric modifications of surfaces⁵. In further analysis, changes in surface mechanical properties could probably be observed due to the asperities self-hardening.

4. Conclusion

The influence of the roughness parameters R_{sk} and R_{ku} for two different machined surfaces was investigated by analyzing the friction and wear coefficients using the pin-on-disc dry sliding wear test. The primary objective of the methodology in obtaining distinct surfaces with similar R_a and R_q parameters was achieved. This made it possible to direct the tribological study towards the parameters of skewness and kurtosis. The milled surface showed 50% less R_{sk} in relation to the turned surface, indicating less peaks. It is also worth mentioning the interesting occurrence of both surfaces having statistically similar kurtosis, despite the fact that it made discussion about tribological behavior impossible.

Different behaviors of the initial friction coefficient were observed and soon afterwards, its stabilization, making it possible to distinguish the phases of running-in and steady regime. Of the three sliding tracks, radius 23 (R23) and 13 (R13) showed a lower friction coefficient for the milled surface compared to the turned surface, with a percentage difference of 9% and 2% respectively. Associating the results with the other studies carried out, it was possible to verify that surfaces whose roughness profile has less high peaks may have a greater capacity to retain particles that could act at the interface as a third body in the tribological system.

The calculated wear coefficients showed magnitudes below the ones considered as “moderate wear” in the literature. There was no significant difference in K in relation to surfaces. Possibly the results of the wear coefficient would be related to the indirect determination of the worn out volume through the loss of mass of the bodies. The reduction in mass was very small in relation to the total mass of the discs, and possibly

the resolution of the precision balance was not sufficient to measure the actual mass.

It was also observed that the feed marks orientation of the machining process in relation to the sliding direction of the pin could have interfered in the behavior of the friction and wear coefficient. When the asperities follow the same direction of the sliding, the contact surface of the pin is probably sustained constantly by a support length, similar to a guide rail. As the sliding time increases, the width of the “rail” increases (flattening of the asperities), thus increasing the friction coefficient, which would be greater in relation to the milled surface where the contact would prevail intermittently, since the orientation of the “rail” “Does not remain constant.

The SEM and EDS analysis on the pins of the R13 tracks show a greater presence of oxides acting on the tribosystem composed of the milled surface and, at the same time, a greater contact area at the interface, possibly due to the feed marks orientation of the machining process. The results served as an indication of the wear and tear on the tracks subsequently analyzed. The width of the tracks presented a correlation with the magnitude of the wear of the pins. F13 and T13 tracks showed values of approximately 255.4 μm and 170.5 μm , respectively. In general observation it was possible to notice the predominance of different wear mechanisms between the surfaces. In track F13 the wear showed an abrasive predominance, characterized by the groove oriented in the direction of the relative movement between the surfaces. In track T13, plastic deformation and adhesion were the predominant mechanisms. Adding to the general results of the friction coefficient, the difference in the skewness parameter R_{sk} and the discussion held about the feed marks orientation in relation to the sliding, it was possible to verify the trend of a better tribological behavior of the milled surface compared to the turned surface.

5. Acknowledgements

The authors are grateful for the support offered by the institutions: Centro Federal de Educação Tecnológica de Minas Gerais, Universidade Federal de Minas Gerais, Centro Universitário UNA and Pontifícia Universidade Católica de Minas Gerais. In particular, thanks to professors Marcelo Araújo Câmara and Alexandre Mendes Abrão, from the Universidade Federal de Minas Gerais, for the idealization of this study.

6. References

1. ASM International Handbook Committee. ASM Handbook: friction, lubrication, and wear technology. United States of America: ASM International; 1992.
2. Bhushan B. Introduction to tribology. New York: John Wiley & Sons; 2013.
3. Hutchings I, Shipway P. Tribology: friction and wear of engineering materials. United States: Elsevier; 2017.
4. Holmberg K, Matthews A. Coatings tribology: properties, mechanisms, techniques and applications in surface engineering. Great Britain: Elsevier; 2009.
5. Barakat H, Zedan Y, Samuel AM, Doty HW, Valtierra S, Samuel FH. Effect of metallurgical parameters on the drilling and tapping characteristics of aluminum cast alloys. Int J Adv Manuf Technol. 2019;105:1357-70.

6. Blau PJ. Friction science and technology: from concepts to applications. New York: CRC Press Taylor & Francis Group; 2009.
7. Haleel AJ. Optimization drilling parameters of aluminum alloy based on taguchi method. *Al-Khwarizmi Engineering Journal*. 2018;14:14-21.
8. Pereira RBD, Silva LA, Lauro CH, Brandão LC, Ferreira JR, Davim JP. Multi-objective robust design of helical milling hole quality on AISI H13 hardened steel by normalized normal constraint coupled with robust parameter design. *Appl Soft Comput*. 2019;75:652-85.
9. He X, Liao W, Wang G, Zhong L, Li M. Evaluation of hydrodynamic lubrication performance of textured surface from the perspective of skewness and kurtosis. *Ind Lubr Tribol*. 2018;70:829-37.
10. Dzierwa A. Influence of surface preparation on surface topography and tribological behaviours. *Archives of Civil and Mechanical Engineering*. 2017;17:502-510.
11. Pelcastre L, Hardell J, Courbon C, Prakash B. Tribological behaviour of Al-Si-coated ultra-high-strength steel during interaction with tool steel at elevated temperatures: influence of tool steel surface topography parameters on galling. *Proc IMechE Part B: J Engineering Manufacture*. 2015;229:1373-84.
12. Todorovic P, Tadic B, Vukelic D, Jeremic M, Randjelovic S, Nikolic R. Analysis of the influence of loading and the plasticity index on variations in surface roughness between two flat surfaces. *Tribol Int*. 2015;81:276-82.
13. García-Jurado D, Vazquez-Martinez JM, Gámez AJ, Batista M, Puerta FJ, Marcos M. FVM based study of the Influence of Secondary Adhesion Tool Wear on Surface Roughness of dry turned Al-Cu aerospace alloy. *Procedia Eng*. 2015;132:600-7.
14. Leach RK. Measurement good practice guide: the measurement of surface texture using stylus instruments. United Kingdom: National Physical Laboratory; 2011.
15. Horváth R, Drégelyi-Kiss Á, Mátyási G. The examination of surface roughness parameters in the fine turning of hypereutectic aluminium alloys. *U.P.B. Sci. Bull., Series D*. 2015;77:205-16.
16. Liang G, Schmauder S, Lyu M, Schneider Y, Zhang C, Han Y. An investigation of the influence of initial roughness on the friction and wear behavior of ground surfaces. *Materials (Basel)*. 2018;11:1-22.
17. Sedláček M, Podgornik B, Vižintin J. Correlation between standard roughness parameters skewness and kurtosis and tribological behaviour of contact surfaces. *Tribol Int*. 2012;48:102-12.
18. Stout K. How smooth is smooth?: Surface measurements and their relevance in manufacturing. *The Production Engineer*. 1980;59(5):17-22. MACH 80 Special Report. <http://dx.doi.org/10.1049/tpe.1980.0076>.
19. Whitehouse DJ. Surface metrology. *Meas Sci Technol*. 1997;8:955-72.
20. To D, Umezawa O, Shinohara T. Detection of surface roughness evolution of carbon steel subjected to outdoor exposure and constant humidity corrosion tests. *Mater Trans*. 2018;59:1239-43.
21. Machado ÁR, Abrão AM, Coelho RT, Silva MB. Teoria da usinagem dos materiais. São Paulo: Editora Blucher; 2009.
22. Sedláček M, Vilhena LMS, Podgornik B, Vižintin J. Surface topography modelling for reduced friction. *Strojniški Vestnik*. 2011;57(9):674-680.
23. Sedláček M, Gregorčič P, Podgornik B. Use of the roughness parameters ssk and sku to control friction: a method for designing surface texturing. *Tribol Trans*. 2016;60:260-6.
24. Shi X, Wang L, Qin F. Relative fatigue life prediction of high-speed and heavy-load ball bearing based on surface texture. *Tribol Int*. 2016;101:364-74.
25. Dzierwa A. Effects of surface preparation on friction and wear in dry sliding conditions. *Tribologia*. 2017;272(2):25-31.
26. Grabon W, Pawlus P, Wos S, Koszela W, Wieczorowski M. Effects of honed cylinder liner surface texture on tribological properties of piston ring-liner assembly in short time tests. *Tribol Int*. 2017;113:137-48.
27. Yuan S, Huang W, Wang X. Orientation effects of micro-grooves on sliding surfaces. *Tribol Int*. 2011;44:1047-54.
28. Wassennan L. All of statistics: a concise course in statistical inference. New York: Springer Science/Business Media, LLC; 2004.
29. ASTM International. ASTM G99-05 - Standard Test Method for Wear Testing with a Pin-on-Disk Apparatus. West Conshohocken: ASTM International; 2010. p. 1-5.
30. Dzierwa A, Pawlus P, Zelasko W. The influence of disc surface topography after vapor blasting on wear of sliding pairs under dry sliding conditions. *Coatings*. 2020;10:1-13.
31. Sedláček M, Podgornik B, Vižintin J. Planning surface texturing for reduced friction in lubricated sliding using surface roughness parameters skewness and kurtosis. *Proc Inst Mech Eng, Part J J Eng Tribol*. 2012;226:661-7.
32. Pinheiro JM, Salústio S, Valente AA, Silva CM. Adsorption heat pump optimization by experimental design and response surface methodology. *Appl Therm Eng*. 2018;138:849-60.
33. Barányi I. Characterization of tribological behaviour of surface topographies by roughness measurement at the beginning of the wear process. *Acta Technica Jaurinensis*. 2020;13:151-60.
34. Horváth R, Czifra Á, Drégelyi-Kiss Á. Effect of conventional and non-conventional tool geometries to skewness and kurtosis of surface roughness in case of fine turning of aluminium alloys with diamond tools. *Int J Adv Manuf Technol*. 2015;78:297-304.
35. Limandri S, Josa VG, Valentini MC, Chen ME, Castellano G. 3D scanning electron microscopy applied to surface characterization of fluorosed dental enamel. *Micron*. 2016;84:54-60.
36. Zmitrowicz A. Wear debris: a review of properties and constitutive models. *J Theor Appl Mech*. 2005;43:3-35.
37. Yan XL, Wang XL, Zhang YY. Influence of roughness parameters skewness and kurtosis on fatigue life under mixed elastohydrodynamic lubrication point contacts. *J Tribol*. 2014;136:031503.
38. Zhang S, Wang W, Zhao Z. The effect of surface roughness characteristics on the elastic-plastic contact performance. *Tribol Int*. 2014;79:59-73.
39. Ghosh A, Sadeghi F. A novel approach to model effects of surface roughness parameters on wear. *Wear*. 2015;338-339:73-94.
40. Charsetad H, Khorsandijou SM. Effect of surface roughness on steel-steel dry friction coefficient. *Journal of Mechanical Research and Application*. 2013;4:45-56.
41. Moronuki N, Furukawa Y. Frictional properties of the micro-textured surface of anisotropically etched silicon. *CIRP Ann - Manuf Technol*. 2003;52:471-474.
42. Pettersson U, Jacobson S. Friction and wear properties of micro textured DLC coated surfaces in boundary lubricated sliding. *Tribol Lett*. 2004;17:553-9.
43. Souza PS, Santos AJ, Cotrim MAP, Abrão AM, Câmara MA. Analysis of the surface energy interactions in the tribological behavior of AlCrN and TiAlN coatings. *Tribol Int*. 2020;146:1-13.
44. Show BK, Mondal DK, Maity J. Dry sliding wear behavior of aluminum-based metal matrix composites with single (Al₂O₃) and hybrid (Al₂O₃ + SiC) reinforcements. *Metallogr. Microstruct. Anal*. 2014;3:11-29.